buildings

MDPI

Article

Mechanical Performance and Reliability Analysis of "Structure-Insulation" Integrated Wall Panel under Grain Load

Kewei Chen [1], Zhanjiong Song [1], Yonggang Ding [1,2,*] and Haoran Wang [1,2]

[1] College of Civil Engineering and Architecture, Henan University of Technology, Zhengzhou 450001, China
[2] Henan Key Laboratory of Grain Storage Facility and Safety, Zhengzhou 450001, China
* Correspondence: cedyg@haut.edu.cn

Abstract: As a new type of grain barn wall component, the "Structure-Insulation" integrated wall panel (SIW) has excellent characteristics such as a high-bearing capacity and good insulation performance. In order to study its mechanical properties under grain load, this paper designed three wall panels with different thicknesses, carried out static loading tests on them, studied their cracking and ultimate load, and analyzed the development trend of the wall panel's crack and deflection. In order to study the reliability of wall panels under stochastic conditions, the performance functions of the wall panel under deflection and strength control conditions were established. The reliability analysis was carried out by using the response surface method and finite element software. The sensitivity degree of each random parameter to different performance functions was quantified. The results show that, under the maximum grain load condition, the deflection of the designed specimens is less than $l_0/250$, and the crack width is less than 0.2 mm, both of which meet the requirements of the normal use limit state. The cracking loads of the three specimens are 13.02, 14.75, and 16.49 kN/m^2, respectively, with corresponding crack widths of 0.06, 0.07, and 0.06 mm. The ultimate load is 65.1, 75.52, and 82.47 kN/m^2, with corresponding maximum crack widths of 1.66, 1.60, and 1.61 mm, respectively. The reliability indexes of the deflection and strength of the thinnest specimens are $\beta_1 = 2.60$ and $\beta_2 = 3.26$, respectively, which meet the safety conditions of ductile failure. The parameter affecting the reliability of concrete deflection is the grain gravity density, with a correlation coefficient of -0.707. The parameter affecting the reliability of concrete strength is concrete strength, with a correlation coefficient of 0.935. Combined with the static load test and reliability analysis, the designed wall panel can meet the normal use of grain under full load and has good reliability. Sensitivity analysis can provide a reference for the optimization of practical engineering design.

Keywords: grain barn; "structure-Insulation" integrated wall panel; static load test; reliability; sensitivity

check for updates

Citation: Chen, K.; Song, Z.; Ding, Y.; Wang, H. Mechanical Performance and Reliability Analysis of "Structure-Insulation" Integrated Wall Panel under Grain Load. *Buildings* **2023**, *13*, 1987. https://doi.org/10.3390/buildings13081987

Received: 13 June 2023
Revised: 25 July 2023
Accepted: 2 August 2023
Published: 3 August 2023

Copyright: © 2023 by the authors. Licensee MDPI, Basel, Switzerland. This article is an open access article distributed under the terms and conditions of the Creative Commons Attribution (CC BY) license (https://creativecommons.org/licenses/by/4.0/).

1. Introduction

As a populous country, food storage is an extremely important task for China. Granary is the infrastructure to ensure food security, which is directly related to the national economy and people's livelihood. At present, the most widely used barn type in China is the grain bungalow, which is mostly built with brick walls, as shown in Figure 1a–c [1]. It has the advantages of a short construction cycle and low cost, but the heat insulation performance is poor, which is very unfavorable to the environment of grain storage [2]. Different from general buildings, granaries need to bear both vertical loads and, more importantly, the horizontal lateral pressure generated by the grain [3]. In order to improve its bearing capacity, it is necessary to design a kind of wall component with both stress and insulation [4,5].

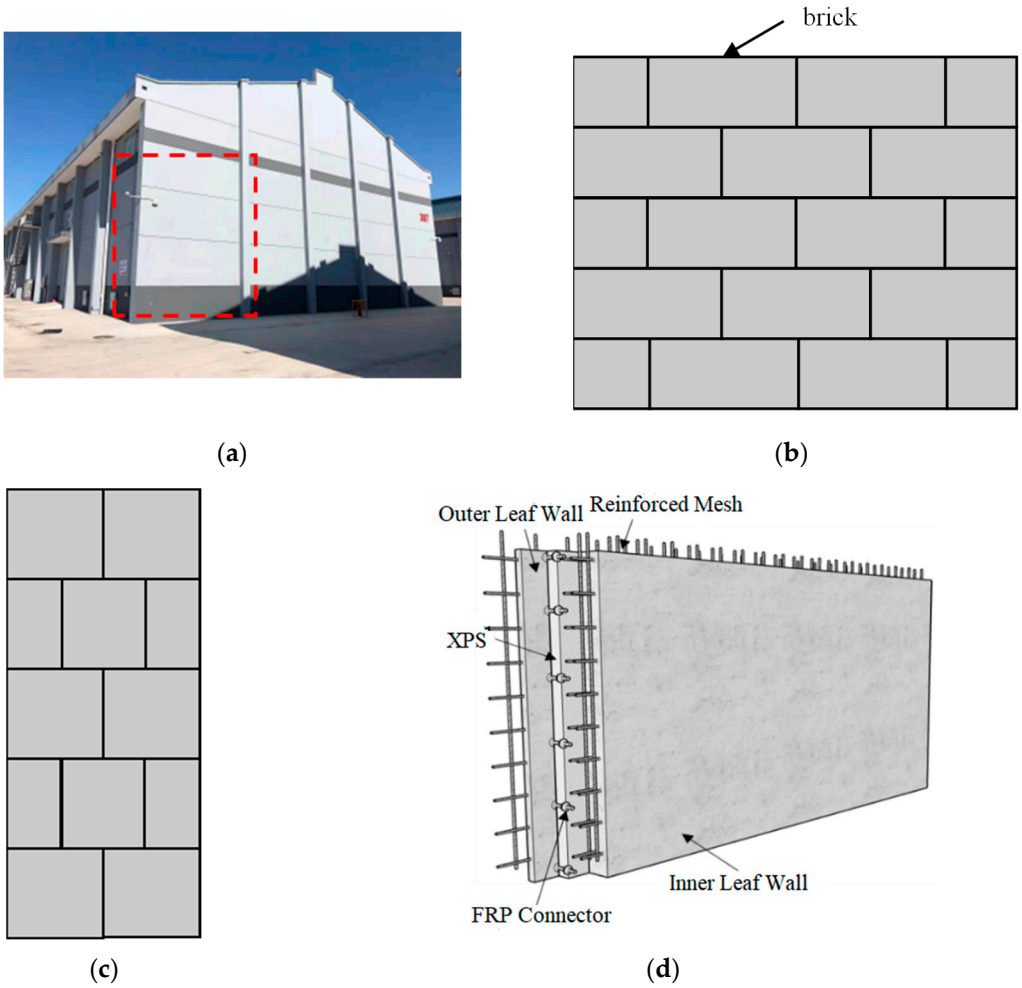


Figure 1. Grain bungalows: (**a**) scene photo; (**b**) traditional brick wall plan; (**c**) traditional brick wall section; (**d**) a new type wall panel.

As the grain barn is relatively tall, this results in larger grain side pressure. But, the traditional brick wall-bearing capacity is insufficient, meaning it often cannot reach the full state, which causes a waste of granary space. Therefore, the granary wall can be a reinforced concrete structure with a high-bearing capacity and good ductility. But, reinforced concrete material is not an excellent insulation material [6,7]. In urban residential buildings, a common way to improve the insulation performance of the wall is to apply a thermal insulation layer on the external wall of the building. However, it may not meet the needs of granaries with higher requirements for insulation performance. Polystyrene resin is a common raw material used for thermal insulation that is easy to process, cheap, and produces extruded polystyrene (XPS) from its processing [8,9]. XPS has a honeycomb structure inside and a high percentage of close pores. The application of XPS in granary walls can effectively improve the grain storage environment. For the composite structure, the connector is an essential part of the combination of different materials, such as XPS [10–12]. Previous studies have shown that glass-fiber-reinforced polymer (GFRP) has high a load-bearing capacity and good heat insulation [13–15]. Therefore, this paper proposes a new type of wall component for grain barns that is composed of inner and outer leaf-reinforced concrete walls and XPS insulation boards as the main components, which are connected using GFRP material. The inner leaf wall is thicker and equipped with two layers of bidirectional steel bars to bear the main load. The outer leaf wall is thin and equipped with single-layer, two-way steel reinforcement, which mainly plays the role of enclosure. XPS is a sandwich material and mainly plays the role of heat preservation and insulation. The construction is shown in Figure 1d.

As a new type of composite structure, its mechanical properties, force morphology, and force transfer mechanism under grain load have not been reported yet. Therefore, it needs to be tested and studied [16–18]. Some scholars have carried out flexural test research on concrete sandwich wall panels with reinforced connectors and found that the failure mode of sandwich wall panels is similar to that of traditional solid reinforced concrete panels. Moreover, a reasonable number of connectors can be configured to realize the joint effect of internal and external wall panels [19–22]. Moreover, some scholars have applied out-of-plane loads to sandwich wall panels by using different connection arrangement methods and found that continuous and segmental configuration methods improve the combination characteristics of the wall panels [23]. Most of them adopt the stepwise loading mode from the loading state to the failure of the specimen so that the changing state of the specimen can be better observed [24].

At present, previous research on composite wall panels is diverse, including seismic performance tests, crack resistance studies, shear performance analysis, crack experimental analysis, and so on [4,25–27]. But, most of them have only analyzed the deterministic value in a single state. As a relatively mature discipline, reliability research can randomize the deterministic environment and analyze certain properties of things with probabilistic results [28]. The safety of granaries is important, and the structure design combined with reliability theory can greatly improve its safety. The new wall panel proposed in this paper is a complex component, involving a variety of materials. If the uncertainty of load, the variability of material properties, and the random dispersion of structure size are not considered, the results of the study will have certain limitations [29–31]. Considering the uncertainty and randomness in the mechanical analysis of the structure, the probability analysis is carried out on the random parameters of the wall panel to study the mechanical reliability performance of the wall panel under the influence of multi-dimensional factors. There are many reliability methods, including the primary second-moment method, the Monte Carlo method, the response surface method, and so on [32–37].

The first-order and second-order moment methods will not converge, and the result is inaccurate when dealing with non-linear functions. The Monte Carlo method needs a large number of samples to ensure the accuracy of results, which consumes much time and money. The response surface method can make the established non-linear function explicit and improve efficiency. Therefore, the response surface method can be used in this paper. On the basis of reliability analysis, sensitivity analysis can be used to study parameters affecting some structural properties [38]. As a structure composed of various materials, the composite wall panel has complex parameter variables. Through sensitivity analysis, parameters with a large influence are obtained. Therefore, their scattered randomness should be emphasized in the construction design [39]. Meanwhile, different parameters have different tendencies to affect the structure. The positive and negative sensitivity represents whether it is beneficial to the structure's performance. Sensitivity-based results provide guidance for optimizing structural parameters [40–42].

Therefore, this paper studies the mechanical characteristics of wall panels under grain load by carrying out a static load test. Based on reliability theory, the parameters are randomized to analyze the reliability performance of wall panels under different control conditions of deflection and strength. The influence of random input parameters on the mechanical properties of wall panels is quantified. Moreover, it provides theoretical support for the design, application, and optimization of actual engineering structures.

2. Materials and Methods (Static Loading Test of "Structure-Insulation" Integrated Wall Panel)

2.1. Test Piece Design

The size of the test piece designed for this test is 2400 mm × 2400 mm. The specific structure is shown in Figure 2. A total of 3 test pieces are designed and named SIW-1, SIW-2, and SIW-3. The difference between them is that the thickness of the inner blade wall mainly bearing the grain load is different, which is 85, 100, and 115 mm, respectively

(NT is used in Figure 2). The thickness of the outer leaf wall is 40 mm, the thickness of the insulation board is 30 mm, and the section size of the connector is 6 mm × 10 mm. The concrete material is C30, and the reinforcement is HRB400 [43,44]. The diameter of the two-way reinforcement for the two layers configured for the inner leaf wall is 8 mm. The diameter of the two-way reinforcement for a single layer configured for the outer leaf wall is 6 mm.

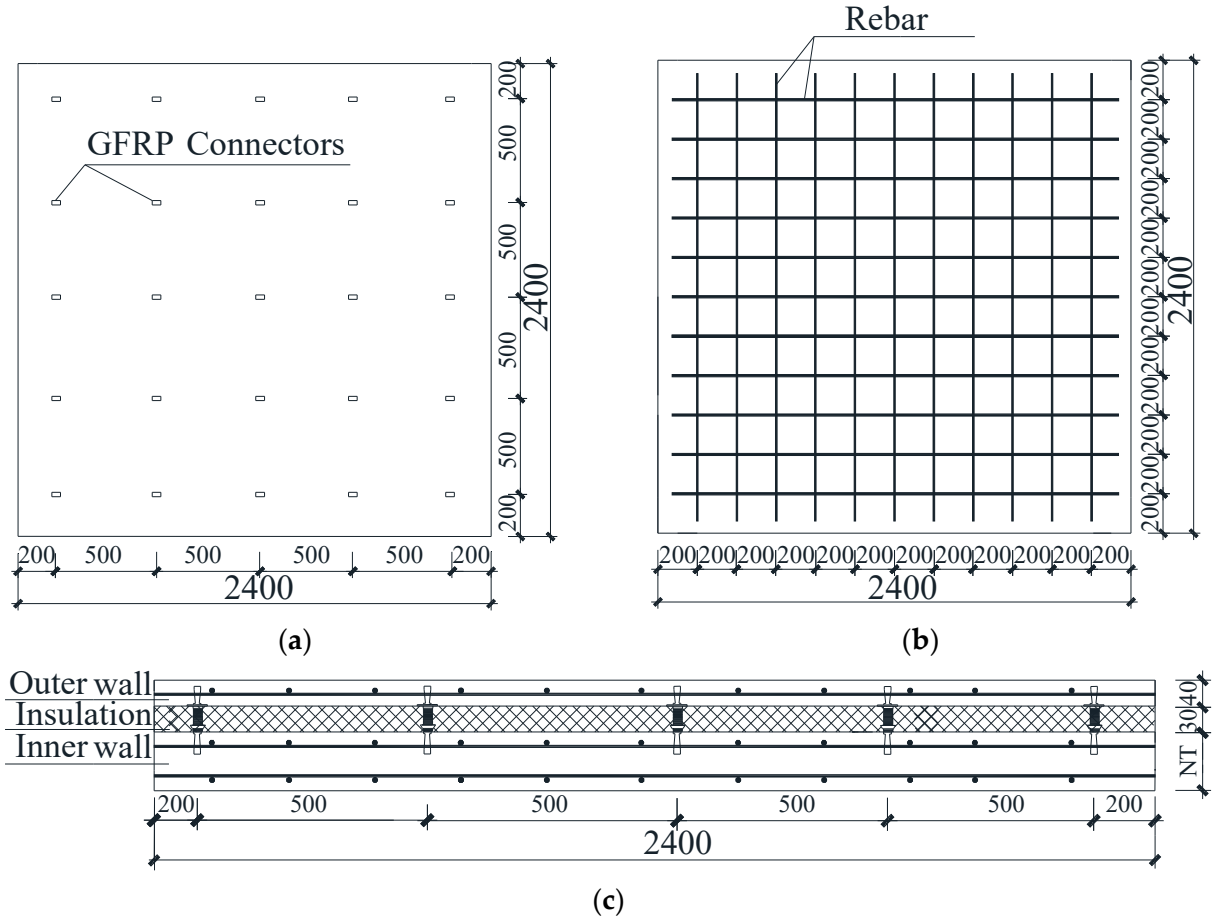


Figure 2. Internal structure and reinforcement of wall panel: (**a**) plan; (**b**) reinforcement; (**c**) section.

2.2. Test Plan

According to GB50320-2014 *Code for Design of Grain Storehouses* [44], the formula for calculating the maximum horizontal lateral pressure of flat bulk grain on the granary wall is

$$P_h = k\gamma s \quad (1)$$

where P_h is the lateral pressure of grain level (kN/m^2); k is pressure coefficient, 0.3562; γ is grain gravity density (kN/m^3), 8 kN/m^3; s is the distance from the top surface of grain to the calculated cross-section (m), and the height of grain loading is 7.2 m. Through calculation, the maximum lateral pressure of grain when the warehouse is full is 20.52 kN/m^2.

This test adopted the loading reaction frame device. Firstly, the specimen was placed horizontally on the support. The jacks then applied an out-of-plane concentrated load to the wall panel. The concentrated load was transformed into the line load through the distribution beam, and the line load was transformed into the distributed load through the steel plate. In addition, 30 mm thick coarse sand was tiled between the specimen and the steel plate to transfer the distributed load to the specimen. The dead weight of the distribution beam, steel plate, and coarse sand is included in the loading process. The

overall effect is shown in Figure 3, and the actual test-loading device is shown in Figure 4. Five percent of the predicted failure load was applied to each stage by using a stepwise loading method. When the specimen was cracked, the loading amount of each stage was increased to 10%. The crack width was delineated and measured for each level of loading.

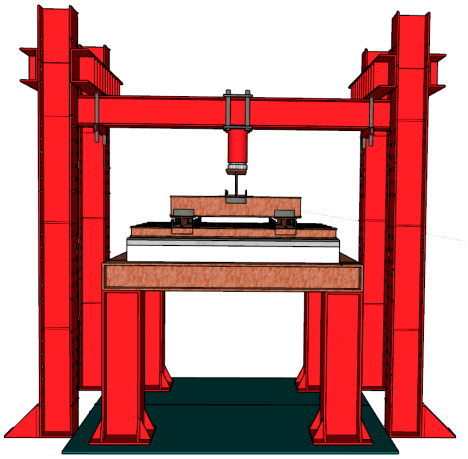


Figure 3. Overall effect.

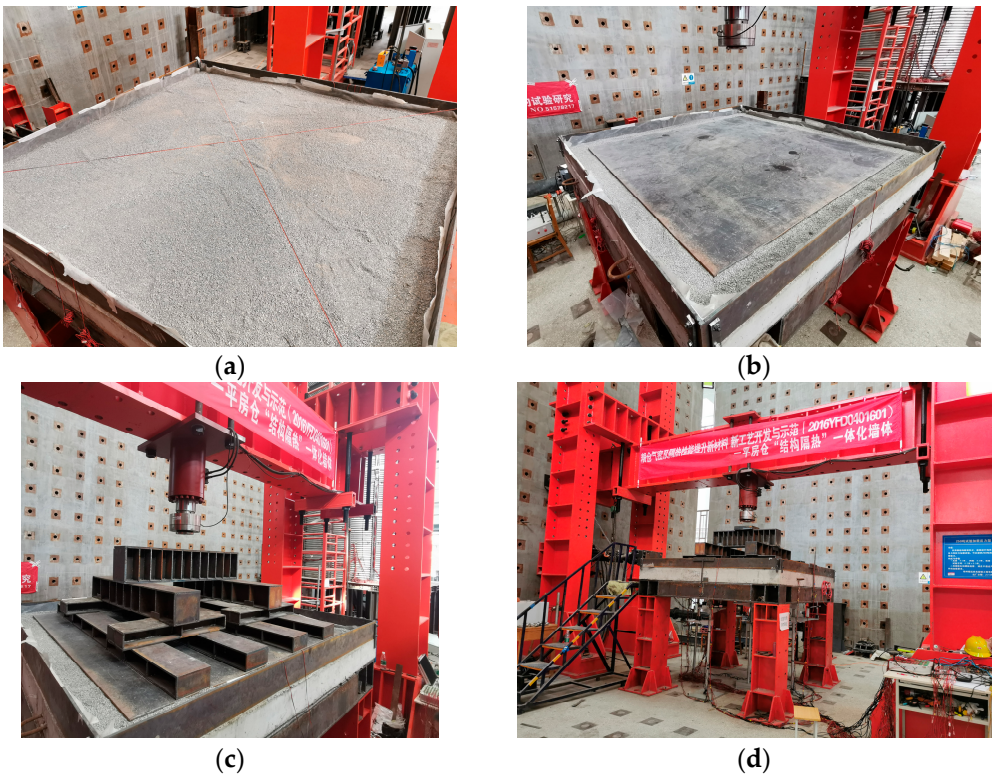


Figure 4. Test loading device: (**a**) laying coarse sand; (**b**) laying steel plate; (**c**) distribution beam; (**d**) actual test.

The same displacement measurement points were arranged for the three specimens, as shown in Figure 5. Nine displacement measurement points (W-1~W-9) were set along the middle span, 1/4 span, and support positions in the x and y directions at the bottom of the outer blade wall panel. A displacement measurement point (WN-1) was set at the midspan of the bottom of the inner leaf wall panel. The displacement meter was used to obtain the displacement data of the specimen, and the crack observation instrument was used to observe the development of the crack, as shown in Figures 6 and 7.

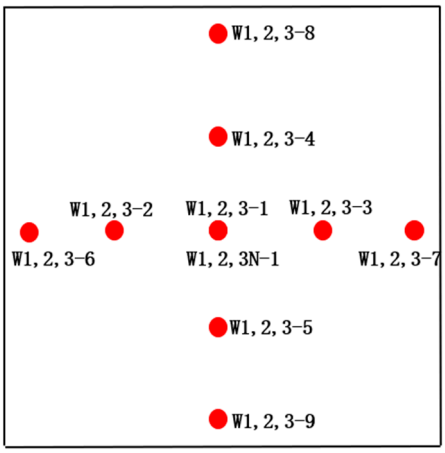


Figure 5. Placement of displacement measurement points.



Figure 6. Displacement meter layout.



Figure 7. Crack observation meter.

2.3. Finite Element Modeling

This analysis was modeled using the finite element software platform. Concrete eight-node hexahedral solid elements with cracks were used for the concrete of the inner and outer leaf walls. The insulation panel uses eight nodes of hexahedral solid elements without cracking. A double node line element was used for the rebar and connector to simulate the actual shape by defining the section size. The maximum grain load is applied to the inner leaf wall directly in contact with the grain using the same loading mode and boundary conditions as the test. The thermal insulation board is bound to the inner and outer leaf walls. Meanwhile, the displacement constraint (x, y, and z directions) is set on the side of the wall panel. The finite element model is shown in Figure 8. According to the analysis in the previous section, the three specimens all meet the limit state of normal

service under the maximum grain load. Therefore, this section only takes the thinnest SIW-1 as an example to carry out reliability analysis.

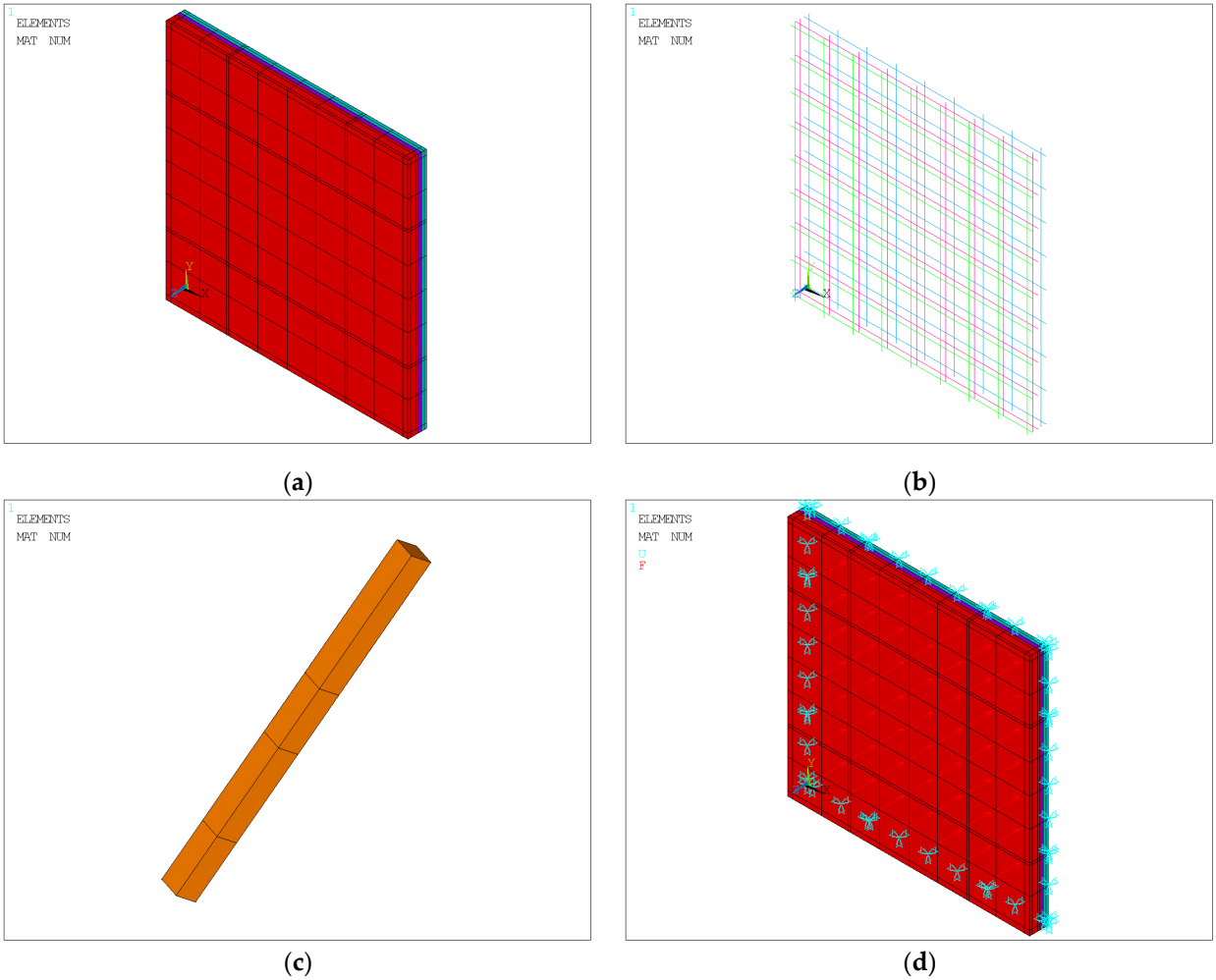


Figure 8. Modeling: (**a**) finite element model; (**b**) reinforcing mesh; (**c**) connector; (**d**) load and boundary condition.

2.4. Reliability Method

The response surface method is a method that obtains certain data using a series of design test methods, as well as multiple quadratic regression equations, to fit the relationship between variables and functions; then, it establishes the approximate function of the original function. In essence, it carries out data fitting through the test sampling method and simplifies the complex finite element model function to the mathematical model function, which makes the implicit equation explicit. Then, enough simulations are performed to increase efficiency and obtain the desired results. In this study, the parameters of the structure are defined as random input variables; random output variables are defined at the same time, and the performance function relationship between random input variables and output variables is established. Sample points and response values are obtained by sampling the input variables several times. Then, the approximate display function of the original function is fitted out, which can transform the finite element model into a mathematically theoretical model and simplify the computational efficiency.

3. Results

The static loading test was carried out in accordance with the requirements of the GB/T50081-2019 *Standard for test methods of concrete physical and mechanical properties* [45]. Three specimens were loaded separately. As shown in Figure 9, the crack development of the three wall panels is measured using the crack observation appearance. The serial number in Figure 9 indicates the sequence of fracture development. It can be seen from Figure 9 that the crack development of the three wall panels is relatively similar, starting from the middle of the span and developing in an X shape, indicating that the wall panels have the characteristics of two-way stress. This is similar to ordinary reinforced concrete two-way slabs, which shows that the structure has good integrity.

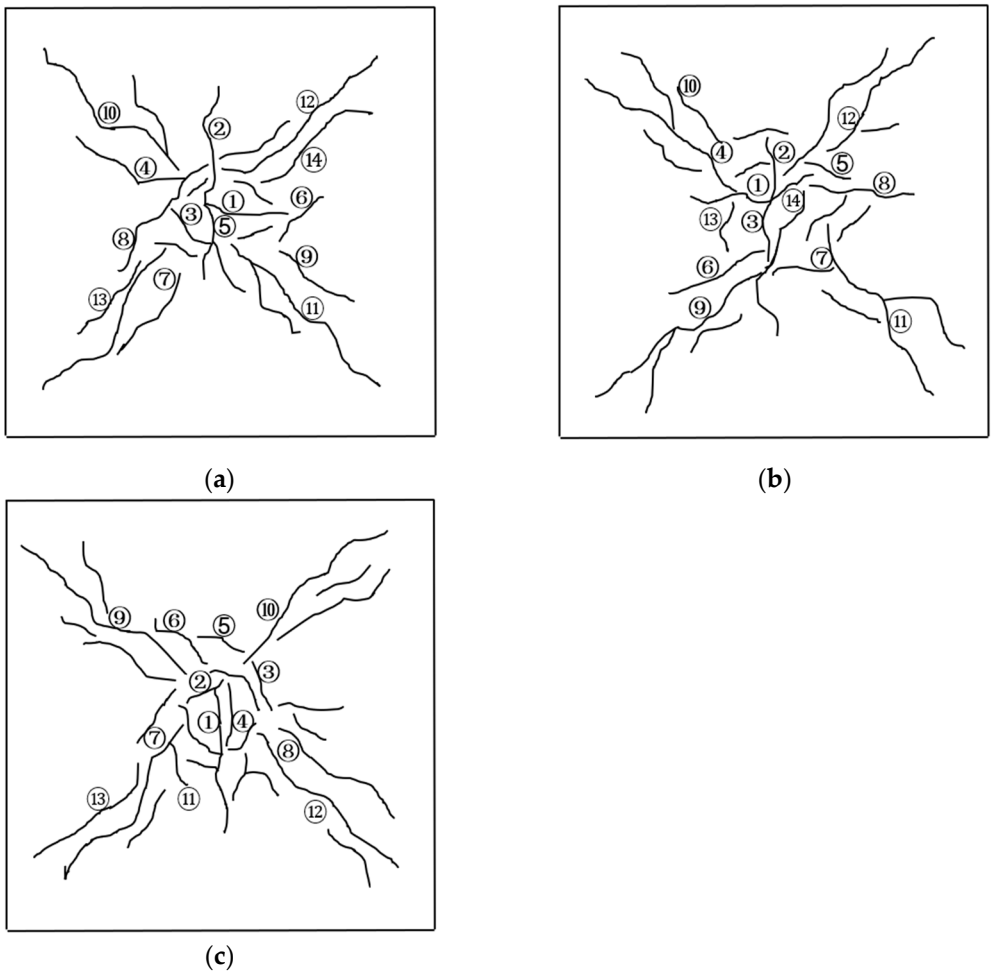


Figure 9. Specimen crack: (**a**) SIW-1 crack; (**b**) SIW-2 crack; (**c**) SIW-3 crack.

Crack widths under various loads were obtained, as shown in Table 1. GB50010-2010 *Code for design of concrete structures* [46] stipulates that 0.2 mm is the crack width of the normal use limit state. When the SIW-1 crack develops to 0.2 mm, the corresponding distributed load is 20.83 kN/m^2, which is greater than the load value of the grain-loading line height of 20.52 kN/m^2, indicating that the wall panel is in a safe state under the maximum load of grain.

Table 1. Crack width under various loads.

Specimen Name	Cracking Load	Maximum Grain Load	Ultimate Load
SIW-1	0.06 mm (13.02 kN/m^2)	0.2 mm (20.83 kN/m^2)	1.66 mm (65.10 kN/m^2)
SIW-2	0.07 mm (14.75 kN/m^2)	0.16 mm (20.83 kN/m^2)	1.60 mm (75.52 kN/m^2)
SIW-3	0.06 mm (16.49 kN/m^2)	0.12 mm (20.83 kN/m^2)	1.61 mm (82.47 kN/m^2)

Using SIW-1 as an example, at the initial stage of loading, the load value is small, and there is no crack at the bottom of the wall panel. The specimen is in the elastic working stage, and the reinforcement and concrete jointly resist the external load. When the distributed load reaches 13.02 kN/m^2, the first visible crack appears at the mid-span of the bottom of the wall panel, which is considered to be the crack load. At this time, the measured crack width is 0.06 mm, and the specimen begins to enter the elastoplastic working state. The generation of cracks results in the stiffness degradation of specimens and the development of cracks begins to accelerate. With the increase in load, new cracks appear continuously after the wall cracking. When the load value reaches 120 kN (converted into a distributed load of 20.83 kN/m^2), the crack width of the specimen reaches 0.2 mm. With the increase in load value, the crack in the midspan part increases continuously. The cracks that have been formed extend further and extend to the four corners, with an angle of about 45° from the edge of the wall panel. When the distributed load reaches 65.1 kN/m^2 and the maximum crack width reaches 1.66 mm (greater than 1.5 mm), reaching the failure condition, it is considered that the specimen reaches the ultimate state of bearing capacity and the loading is finished. During the loading process of the wall panel, there were no phenomena such as the reinforcement being pulled off, the concrete being crushed, and the deflection being too large. The wall panel shows a good feature of cooperative stress. The crack development law of the three specimens is similar. When the wall plate is thicker, the cracking load is larger, the ultimate load is larger, and the bearing capacity is higher.

The load–deflection curves of each measurement point of the three specimens were obtained, as shown in Figure 10. According to the load–deflection curve, it can be seen that the deflection of the wall panel at the midspan position (W-1) is the largest and the deflection near the support is the smallest. At the same time, according to the increasing trend of deflection at the measurement points in different directions, the deformation of the wall panels is symmetric in the x and y directions. Moreover, the three wall panels show similar laws. From the beginning of loading to the appearance of the first crack, the deflection of each measuring point basically shows linear growth. At this time, the specimen is in an uncracked and elastic working stage. After the first crack appears, the specimen begins to enter the stage of elastic–plastic operation with the crack. The slight cracks have little effect on the mechanical properties of the wall panel. The slope of load–deflection curve is slightly reduced, but the inflection point of the curve is not obvious. With the increase in load, the cracks increase gradually, the deflection of the wall panel increases nonlinearly, and the slope of the curve decreases obviously. Then, the specimen enters the plastic stage until the crack width exceeds the limit value, which is regarded as the specimen reaching the ultimate state of bearing capacity. At this stage, the deflection is still increasing, and the specimen exhibits good ductility. Further observation also shows that, under the same load, with an increase in the thickness of the inner leaf wall, the flexural stiffness of the specimen gradually increases and the change of deflection gradually decreases. Moreover, the later the specimen enters the elastic–plastic stage and reaches the failure time, the greater the cracking load and failure load. It can be seen that the increase in inner blade wall thickness has an effect on the bending stiffness, cracking stiffness, and failure load.

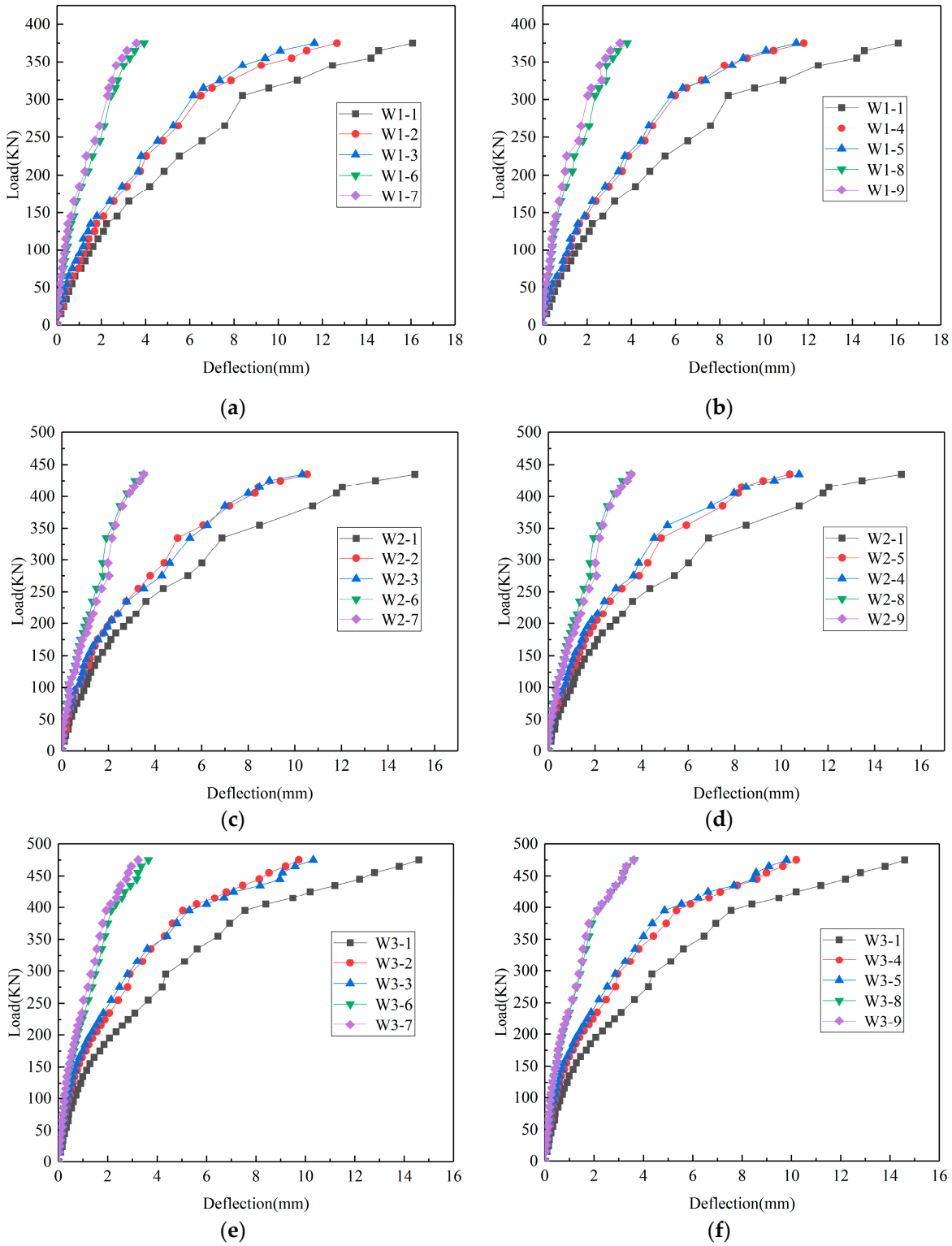


Figure 10. Load–deflection curve: (**a**) SIW-1 (*x* direction); (**b**) SIW-1 (*y* direction); (**c**) SIW-2 (*x* direction); (**d**) SIW-2 (*y* direction); (**e**) SIW-3 (*x* direction); (**f**) SIW-3 (*y* direction).

In addition, under the maximum grain load corresponding to the grainloading height of 7.2 m, the mid-span deflections of the three specimens are 1.99 mm, 1.25 mm, and 0.91 mm, respectively. All of them are less than $l_0/250$, as stipulated in *Code for design of concrete structures*; therefore, it meets the requirements of the normal use limit state.

As shown in Figure 11, according to the deflection change curves at different positions of the three wall panels under various loads (the total load value of the wall panel is obtained by converting the distributed load), it can be seen that, with the increase in load, cracks gradually appear, the deflection changes gradually accelerate, and the midspan part has the largest deflection. Under the action of load, the wall panels and ordinary reinforced concrete two-way panels show similar stress and deformation characteristics. This also shows that the outer blade wall shares part of the load under the force transfer of the connector, exhibiting good integrity. As a whole, the curve is smooth and without obvious mutation, and the whole wall panel shows good bending stiffness.

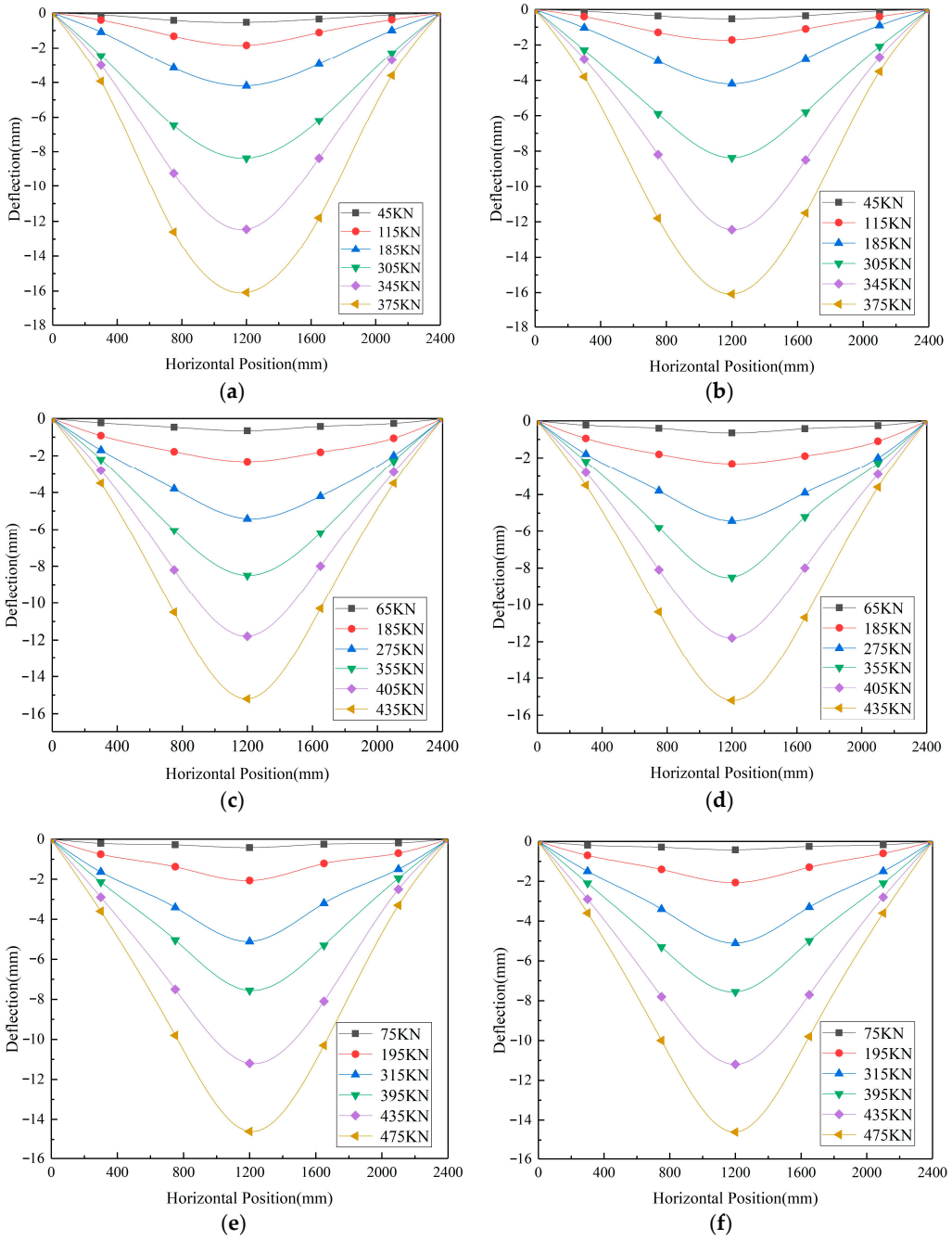


Figure 11. Deflection curve at different positions under different loads: (**a**) SIW-1 (*x* direction); (**b**) SIW-1 (*y* direction); (**c**) SIW-2 (*x* direction); (**d**) SIW-2 (*y* direction); (**e**) SIW-3 (*x* direction); (**f**) SIW-3 (*y* direction).

Meanwhile, the deflection and load curves of the middle span of the inner and outer leaf walls of the three wall panels were drawn, as shown in Figure 12. By comparing the deflection changes, it can be seen that there is not much difference between the two curves. It is therefore proved that the connector can connect the two concrete wall panels, resulting in the co-deformation and joint force of the inner and outer leaf walls, which shows that the wall panel has good integrity.

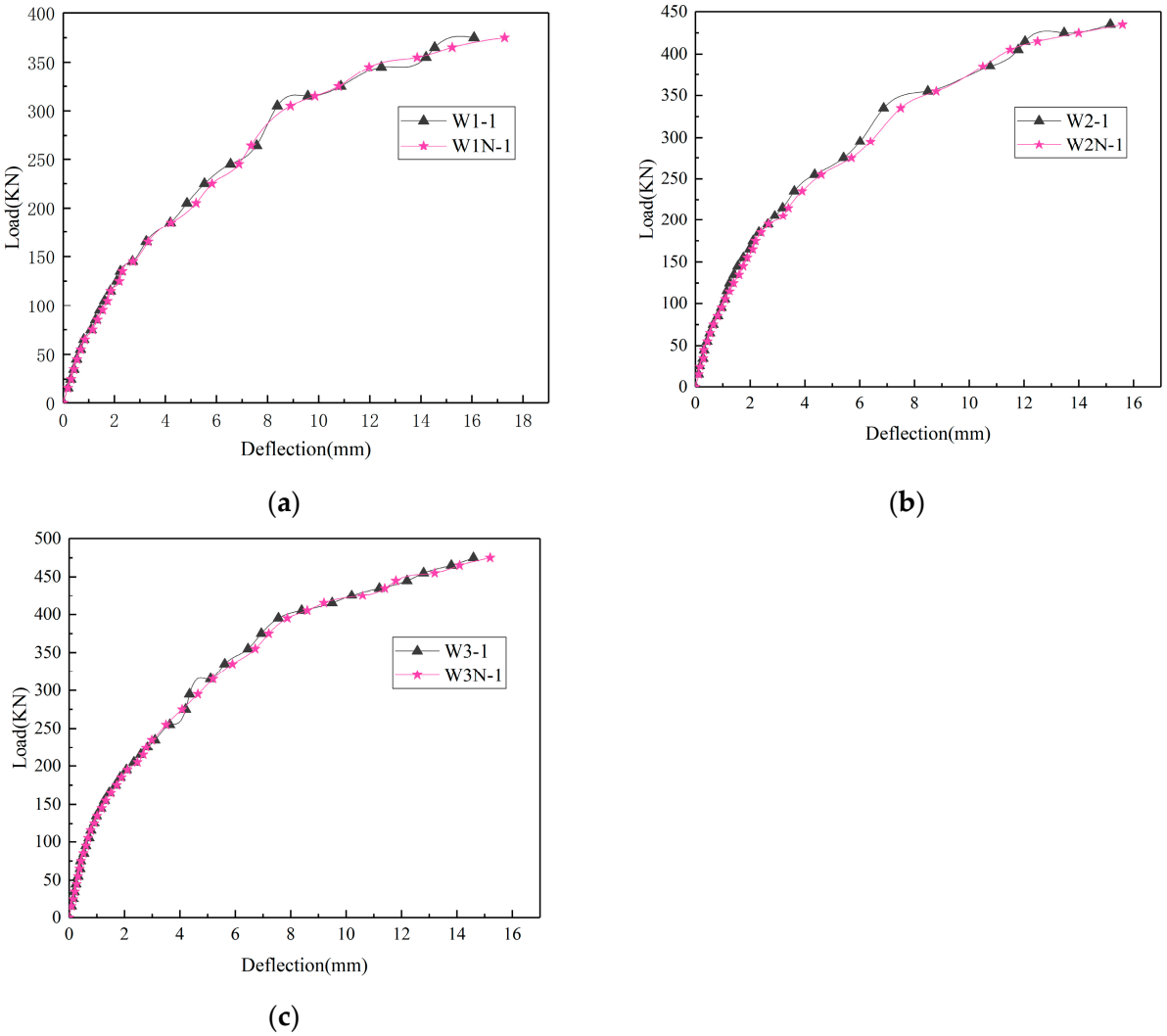


Figure 12. Load–deflection curves at the midspan of inner and outer leaf walls: (**a**) SIW-1; (**b**) SIW-2; (**c**) SIW-3.

Through the analysis of the test results in this section, the cracking loads of the three specimens designed are 13.02, 14.75, and 16.49 kN/m^2, with corresponding crack widths of 0.06, 0.07, and 0.06 mm, respectively. The ultimate loads are 65.1, 75.52, and 82.47 kN/m^2, with corresponding maximum crack widths of 1.66, 1.60, and 1.61 mm, respectively. Under the maximum grain load, all three specimens can meet the requirements of deflection and crack stipulated in the standard. With an increase in load, cracks appear gradually and the change of deflection is accelerated gradually. It is also proved that the connector can connect the two concrete wall panels, resulting in the co-deformation and joint force of the inner and outer leaf walls, which shows that the wall panel has good integrity.

In a previous study, Chen et al. [23] applied external plane loads to sandwich wall panels with FRP plate connectors, and the connectors were arranged in continuous, segmental, and discrete ways, respectively. The results showed that the wall panels exhibit different

degrees of combination. Among them, the combination characteristics of the continuous and segmental arrangement were better, and the combination characteristics of the discrete arrangement were worse. The SIW specimens in this test were also arranged in accordance with continuity and regularity, showing a good combination. Choi et al. [47,48] studied the combined effect of sandwich wall panels equipped with GFRP mesh-type connectors. The results showed that the bonding force between concrete and insulation panels contributed to the combined effect. In addition, the combined effect of the wall panels under the monotonic load was higher than that the under cyclic load. Joseph et al. [4] conducted a bending load test on a one-way sandwich plate with trussed shear connectors. It was found that the number of cracks and crack spacing were affected by the reinforcement volume ratio and the specific surface area of the reinforcement.

The SIW wall panel can have all the above advantages. SIW wall panels are similar to other sandwich composite wall panels in that the connecting parts can well connect the inner and outer leaf walls together, cooperate with the force, and show good mechanical performance. However, there was no sandwich wall specially used for grain bungalows before. In this paper, according to the existing research, a new type of sandwich composite wall panel (SIW) is designed which can effectively bear the action of grain side pressure and has better insulation performance. The experimental study on the mechanical performance of SIW wall panels shows that SIW can bear the grain load under the action of a full warehouse and the cracks and deflections can meet the corresponding specifications.

4. Discussion

4.1. Finite Element Analysis

After applying the load for nonlinear analysis, the load–deflection curve is obtained as shown in Figure 13. It can be seen from Figure 13 that the deflection curve of the simulated load is roughly the same as that of the test load. Due to the errors and the inaccuracy of loading, the test value is small and fluctuates; therefore, it can be regarded as a good simulation situation. It can be seen from the second section that the maximum grain load value is 20.52 kN/m^2 in the full granary. Therefore, the displacement cloud maps of the inner and outer leaf walls under the load of the maximum grain height are obtained as shown in Figure 14. It can be seen from Figure 14 that the simulated deflection of the inner and outer leaf walls are about 2.05 mm and 2.04 mm, respectively.

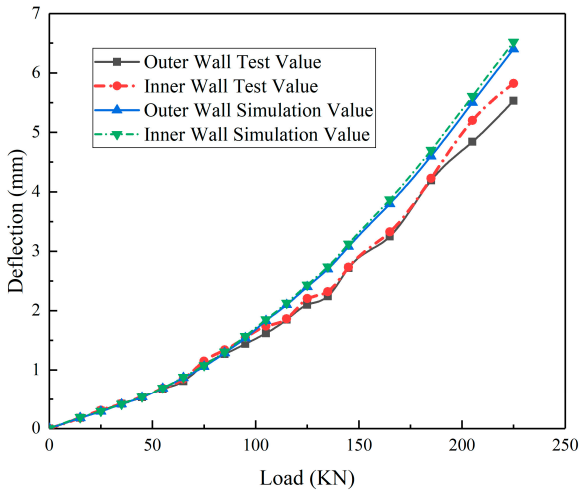
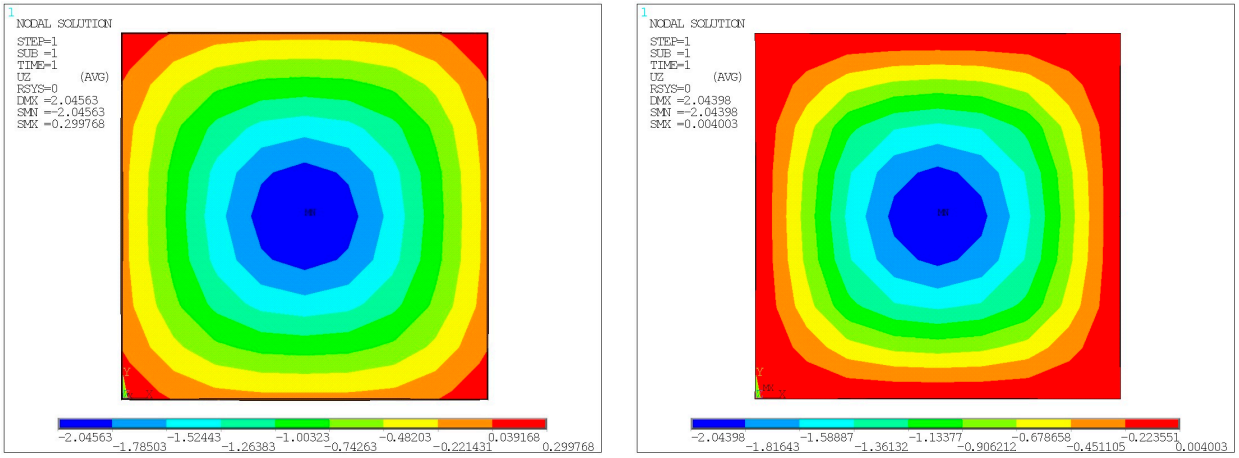


Figure 13. Load deflection curve of SIW-1.



(**a**) (**b**)

Figure 14. Displacement cloud map: (**a**) the inner leaf wall; (**b**) the outer leaf wall.

The deflection of inner and outer leaf wall panels under full grain load is 1.99 mm and 1.96 mm, respectively. Compared with the simulated values, the difference values are 2.9% and 3.9%, which further verifies the accuracy and effectiveness of the model, as can be seen in Figure 15. Based on this model, this chapter carries out the reliability and sensitivity analysis of SIW wall panels under the condition of maximum load of a full grain warehouse.

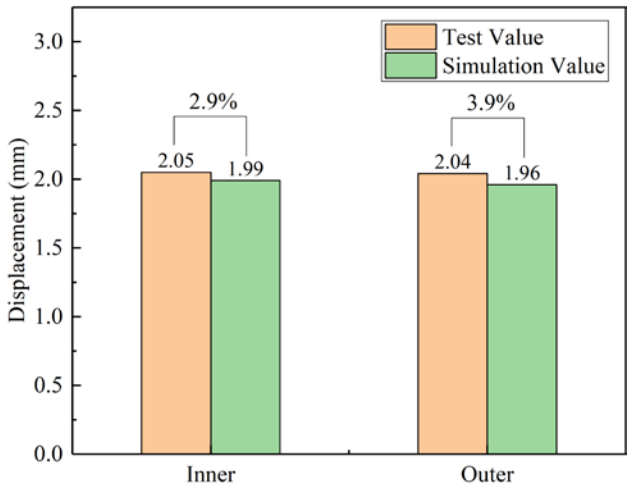


Figure 15. Comparison of simulated values of maximum deflection test.

4.2. Random Sampling

The random values of the input variables affecting the SIW wall panel are shown in Table 2. The values of the coefficient of variation are derived from the relevant literature [49,50] and engineering experience. The mean value is derived from the material property test. Moreover, according to the literature [51], in the case of dead load, random variables generally follow a normal distribution when there is a large amount of data. Since this section considers reliability under the condition of full grain storage, the random variables were set as the normal distribution.

Table 2. Distribution characteristics of random variables.

Random Variable	Average/μ	Coefficient of Variation/δ	Code Name
Grain height (m)	7.2	0.05	H1
Grain density (kN/m^3)	8	0.07	DENS
Thickness of outer leaf wall (mm)	40	0.03	WH
Thickness of insulation panel (mm)	30	0.03	XH
Thickness of inner leaf wall (mm)	85	0.03	NH
Radius of rebar of outer leaf wall (mm)	3	0.03	RAD1
Radius of rebar of inner leaf wall (mm)	4	0.03	RAD2
Section width of connector (mm)	6	0.03	KUAN
Section length of connector (mm)	10	0.03	CHANG
Elastic modulus of outer wall concrete (MPa)	3.01×10^4	0.05	YOUNG1
Elastic modulus of inner wall concrete (MPa)	3.01×10^4	0.05	YOUNG2
Elastic modulus of outer wall rebar (MPa)	2×10^5	0.05	YOUNG3
Elastic modulus of inner wall rebar (MPa)	2×10^5	0.05	YOUNG4
Elastic modulus of inner wall rebar (MPa)	2×10^5	0.05	YOUNG5
Elastic modulus of GFRP connector (MPa)	5.93×10^5	0.05	YOUNG6
C30 concrete compressive strength (N/mm^2)	28.03	0.172	FC

According to *Code for design of concrete structures* [46], the wall panel under the action of the grain side pressure is a flexural member, whose maximum deflection should not exceed the calculated span $l_0/250$, named ω_{lim}. ω_{max} is the maximum deflection obtained by simulation. The deflection function of the SIW wall panel can be established:

$$Z1 = \omega_{\text{lim}} - \omega_{\text{max}} \tag{2}$$

Meanwhile, the strength function of SIW wall panel concrete is established:

$$Z2 = f_c - \sigma_{\text{Mises}} \tag{3}$$

where f_c is the design value of concrete compressive strength and σ_{Mises} is the maximum equivalent stress of concrete.

In this study, the response surface method was used to conduct 10^6 random samples of random input variables. Taking WTH and YOUNG1 as examples, sample values and the distribution histograms of random input parameters are shown in Figure 16. As can be seen from Figure 16a,b, WTH is sampled 10^6 times in total, with an average sampling value of 40 mm, a minimum value of 34.37 mm, and a maximum value of 46.12 mm. Figure 16c,d shows that YOUNG1 is sampled 10^6 times, with an average sampling value of 3.01×10^4 MPa, a minimum sampling value of 2.22×10^4 MPa, and a maximum sampling value of 3.76×10^4 MPa. According to the sample scatter diagram and distribution histogram, there are enough data to support this simulation study. Moreover, these samples have been extracted according to the requirements of Table 2.

4.3. Failure Probability

After the sampling calculation, the cumulative distribution curves of $Z1$ and $Z2$ functions, as shown in Figure 17, are obtained. It can be seen from the figure that the function curve is smooth and has good convergence, indicating that 10^6 times of sampling can meet the data requirements. The failure probability ($P_{f_1} = 4.60 \times 10^{-3}$, $P_{f_2} = 5.58 \times 10^{-4}$) is calculated in the sampling of the two functions, respectively. The reliability indexes are $\beta_1 = 2.60$ and $\beta_2 = 3.26$, respectively. For ductility failure, the GB50068-2018 *Unified standard for reliability design of building structures* [52] requires that, when the design safety level is 2, the reliability index of the normal service limit state should be taken as $\beta > 1.5$; meanwhile, the bearing capacity limit state should be taken as $\beta > 3.2$. Therefore, the reliability of SIW wall panel deflection and concrete strength both meet the safety conditions.

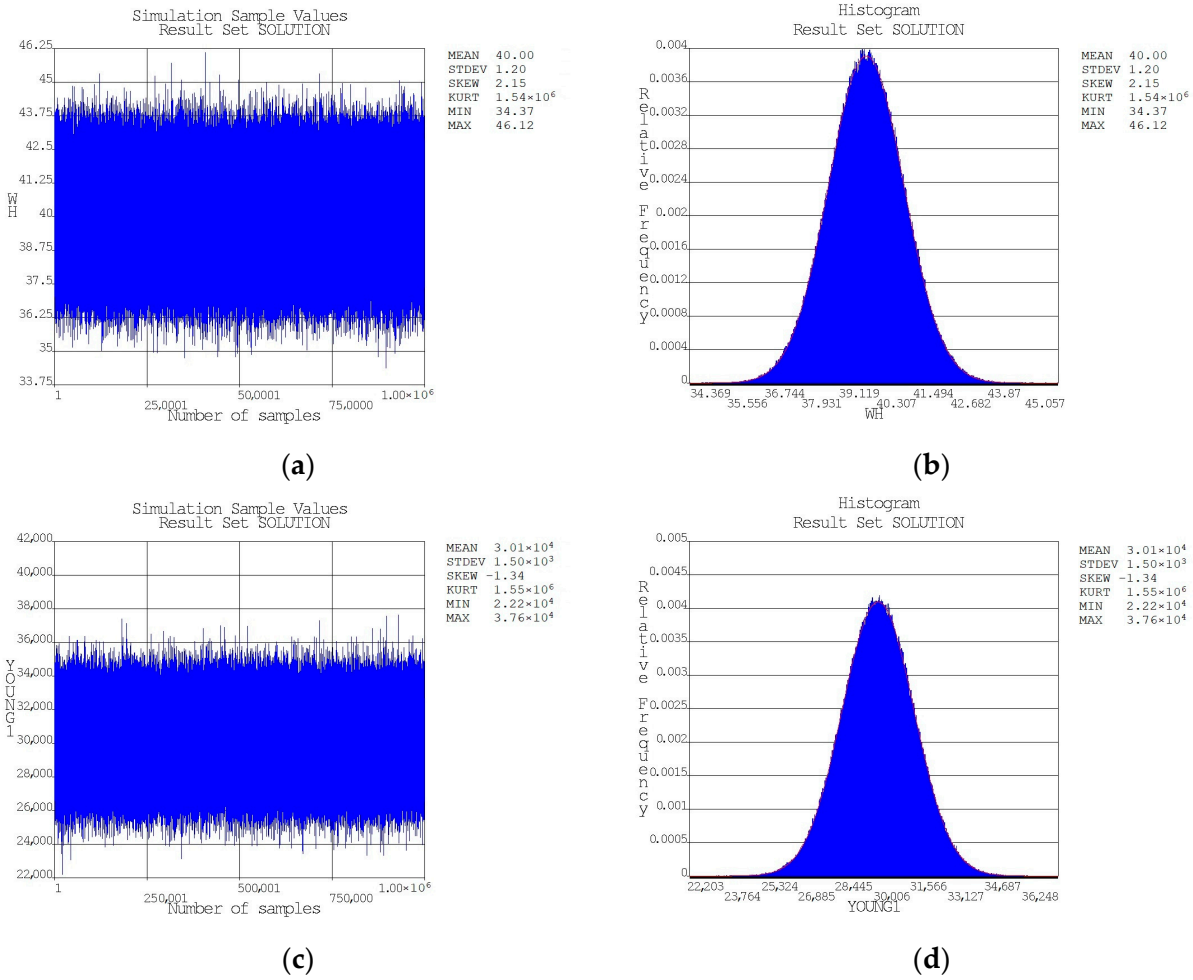


Figure 16. Sampling: (**a**) WTH sample; (**b**) WTH distribution; (**c**) YOUNG1 sample; (**d**) YOUNG1 distribution.

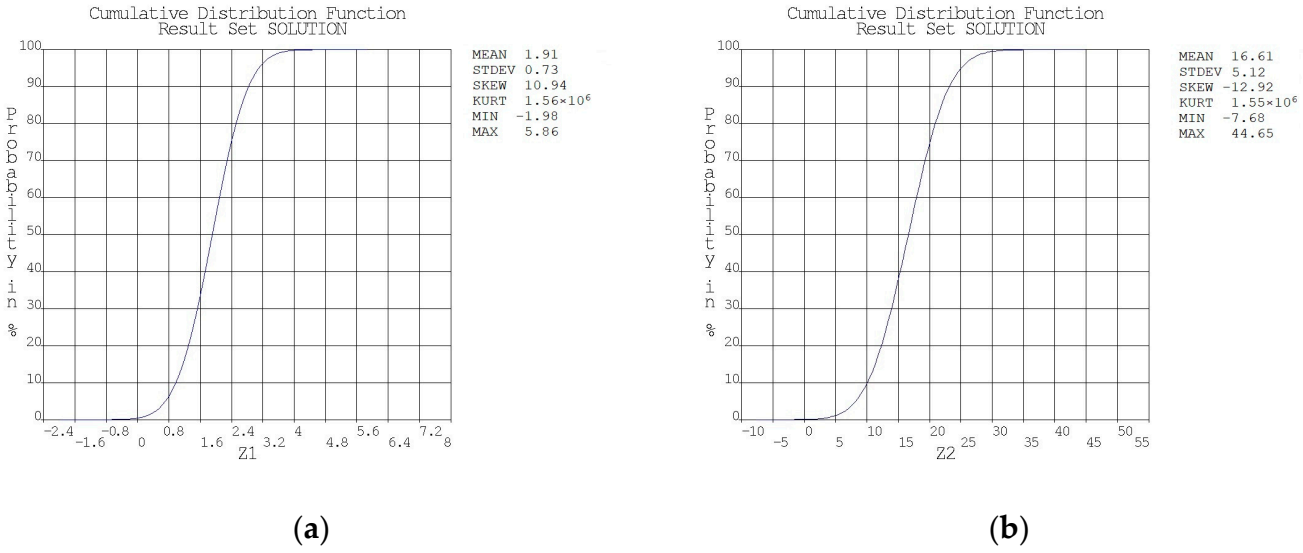
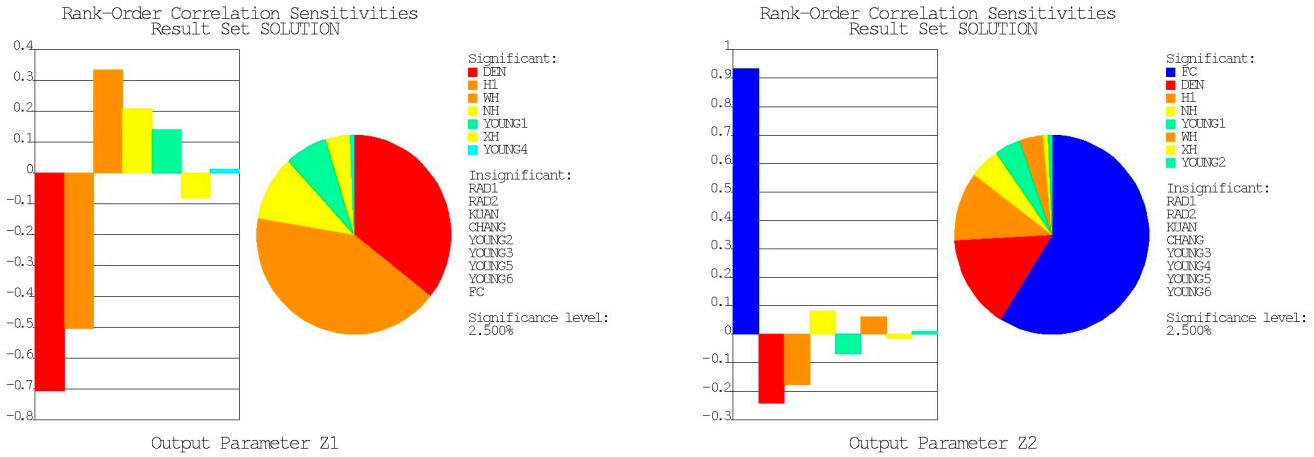


Figure 17. Cumulative distribution curve: (**a**) *Z*1; (**b**) *Z*2.

4.4. Sensitivity Analysis

In addition, the sensitivity of the Z1 and Z2 functions, with respect to random input variables, was obtained, as shown in Figure 18. It can be seen from Figure 18a that the parameters that significantly affect the sensitivity of Z1 (wall panel deflection) are DEN, H1, WH, NH, YOUNG1, XH, and YOUNG4. Among them, WH, NH, YOUNG1, and YOUNG4 have a positive impact on the reliability of concrete deflection, while DEN, H1, and XH have a negative impact on the reliability of concrete deflection. It can be seen from Figure 18b that the parameters that significantly affect the sensitivity of Z2 (concrete strength) are FC, DEN, H1, NH, YOUNG1, WH, XH, and YOUNG2. Among them, FC, NH, WH, and YOUNG2 have a positive impact on the reliability of concrete strength, while DEN, H1, YOUNG1, and XH have a negative impact on the reliability of concrete strength.



(a) **(b)**

Figure 18. Sensitivity: (**a**) Z1; (**b**) Z2.

Then, the correlation coefficients of the Z1 and Z2 functions regarding the random input parameters were obtained and a correlation coefficient table was drawn, as shown in Table 3. Combined with Figure 18 and Table 3, it can be seen that the most significant parameter affecting the reliability of concrete deflection is the grain gravity density DEN, with a correlation coefficient of −0.707. The most significant parameter affecting concrete strength reliability is concrete strength, with a correlation coefficient of 0.935. In the design and manufacture of wall panels, we should focus on the random dispersion of the key parameters to reduce and control their variability as far as possible to ensure the reliable performance of the structure. Meanwhile, the parameter with a positive phase relation value can be appropriately increased, and the parameter with a negative phase relation value can be appropriately reduced, to achieve the purpose of structural optimization.

Table 3. Correlation coefficient.

	DEN	H1	WH	NH	YOUNG1
Z1	−0.707	−0.504	0.334	0.209	0.141
	FC	DEN	H1	NH	YOUNG1
Z2	0.935	−0.242	−0.177	0.081	−0.069

5. Conclusions

A new type of wall panel (SIW) is proposed specially for the wall of grain bungalows. Compared with traditional brick walls, SIW wall panels have a higher carrying capacity, better insulation performance, and more environmentally friendly performance. In order to study the mechanical properties of SIW wall panels under full grain load, a static loading test, reliability analysis, and sensitivity analysis were carried out. The following conclusions are drawn:

(1) Under the maximum grain load corresponding to the grain-loading height of 7.2 m, the mid-span deflections of the three specimens are 1.99 mm, 1.25 mm, and 0.91 mm respectively, which are all less than $l_0/250$. The crack width of the three specimens is less than 0.2 mm, which can meet the requirements of a normal service limit state. With an increase in load, cracks gradually appear, and the deflection changes gradually faster, which is "butterfly-shaped". It is also proved that the connector can connect the two concrete wall panels, resulting in the co-deformation and joint force of the inner and outer leaf walls, which shows that the wall panel has good integrity;

(2) The cracking loads of the three specimens are 13.02, 14.75, and 16.49 kN/m^2, respectively, with corresponding crack widths of 0.06, 0.07, and 0.06 mm, respectively. The ultimate loads are 65.1, 75.52, and 82.47 kN/m^2, respectively, with corresponding maximum crack widths of 1.66, 1.60, and 1.61 mm, respectively;

(3) By 10^6 sample simulations, the failure probabilities of deflection and strength functions are $P_{f_1} = 4.60 \times 10^{-3}$ and $P_{f_2} = 5.58 \times 10^{-4}$, which are converted into reliability indexes $\beta_1 = 2.60$ and $\beta_2 = 3.26$, respectively. All of them meet the safety conditions of ductile failure;

(4) The parameter that has the greatest influence on the reliability of concrete deflection is the grain gravity density, with a correlation coefficient of -0.707. The parameter that has the greatest influence on the reliability of SIW wall panel concrete stress is the concrete compressive strength, with a correlation coefficient of 0.935.

The research shows that the wall panel designed in this paper has good mechanical reliability performance. According to the results of the sensitivity analysis, the structural design parameters can be better optimized in combination with engineering applications, which provide a theoretical basis for the application of the new wall structure for granaries.

Author Contributions: Conceptualization, K.C. and Y.D.; methodology, Z.S.; software, K.C.; validation, Z.S. and H.W.; formal analysis, K.C.; investigation, K.C.; resources, Z.S.; data curation, H.W.; writing—original draft preparation, K.C.; writing—review and editing, Z.S.; visualization, K.C.; supervision, Y.D.; project administration, H.W.; funding acquisition, Y.D. All authors have read and agreed to the published version of the manuscript.

Funding: This research was funded by the National Natural Science Foundation of China (Grant No. 2016YFD0401601).

Data Availability Statement: The data used to support the findings of this study are available from the corresponding author upon request.

Conflicts of Interest: The authors declare no conflict of interest.

References

1. Chen, H.; Wei, K.; Wang, Y. The present situation and development of new warehouse types of grain reserves in China. *Farm Mach.* **2013**, *1*, 67–70. [CrossRef]
2. Jia, J.F.; He, W. Study on heat insulation performance of external wall of low temperature grain storage granary. *Adv. J. Food Sci. Technol.* **2015**, *8*, 306–311. [CrossRef]
3. Yu, X.; Raeesi, A.; Ghaednia, H.; Heydariha, J.; Das, S.; Xie, S. Behavior of a large steel field silo structure subject to grain loading. *J. Perform. Constr. Facil.* **2017**, *31*, 04017038. [CrossRef]
4. Joseph, J.; Prabakar, J.; Alagusundaramoorthy, P. Precast concrete sandwich one-way slabs under flexural loading. *Eng. Struct.* **2017**, *138*, 447–457. [CrossRef]
5. Wang, W.; Ma, J. Performance analysis on improvement of the heat insulation of grain storehouse. *Appl. Mech. Mater.* **2011**, *71*, 193–196. [CrossRef]

6. Wi, S.; Ji, H.P.; Kim, Y.U.; Yang, S.; Kim, S. Thermal, hygric, and environmental performance evaluation of thermal insulation materials for their sustainable utilization in buildings. *Environ. Pollut.* **2020**, *272*, 116033. [CrossRef]
7. Durakovic, B.; Yildiz, G.; Yahia, M.E. Comparative performance evaluation of conventional and renewable thermal insulation materials used in building envelops. *Teh. Vjesn. Tech. Gaz.* **2020**, *27*, 283–289. [CrossRef]
8. Yoo, J.; Chang, S.J.; Yang, S.; Wi, S.; Kim, S. Performance of the hygrothermal behavior of the CLT wall using different types of insulation; XPS, PF board and glass wool. *Case Stud. Therm. Eng.* **2021**, *24*, 100846. [CrossRef]
9. Li, X.; Peng, C.; Liu, L. Experimental study of the thermal performance of a building wall with vacuum insulation panels and extruded polystyrene foams. *Appl. Therm. Eng.* **2020**, *180*, 115801. [CrossRef]
10. Wei, Y.; Chen, S.; Jiang, J.; Zhou, M.; Zhao, K. Experimental investigation of bamboo-concrete composite beams with threaded reinforcement connections. *J. Sandw. Struct. Mater.* **2021**, *24*, 601–626. [CrossRef]
11. Ding, C.; Bai, Y.; Yang, K.; Zhang, J. Cyclic behaviour of prefabricated connections for steel beam to concrete filled steel tube column. *J. Constr. Steel Res.* **2021**, *176*, 106422. [CrossRef]
12. Bai, F.; Sun, Y.; Liu, X.; Li, X. A theoretical perspective on the effective distribution of shear connectors in sandwich structures. *Compos. Struct.* **2021**, *272*, 114139. [CrossRef]
13. Zhang, X.; Kong, W.; Zhu, Y.; Chen, Y. Investigation on various section GFRP profile strengthening concrete-filled GFRP tubular columns. *Compos. Struct.* **2021**, *283*, 115055. [CrossRef]
14. Li, S.; Wang, H.; He, H.; Liu, Y.; Fan, H. Experimental investigation of mechanical behaviors of EPS foamed concrete-filled pultruded GFRP sandwich panels. *Polym. Test.* **2021**, *104*, 107401. [CrossRef]
15. Borri, A.; Corradi, M.; Sisti, R.; Buratti, C.; Belloni, E.; Moretti, E. Masonry wall panels retrofitted with thermal-insulating GFRP-reinforced jacketing. *Mater. Struct.* **2016**, *49*, 3957–3968. [CrossRef]
16. Mostafa, A. Experimental and numerical investigation on enhancing the structural integrity of composite sandwich structure. *Adv. Struct. Eng.* **2019**, *22*, 2149–2162. [CrossRef]
17. Kwak, B.S.; Kim, H.I.; Dong, S.J.; Choi, J.H.; Kweon, J.H. An experimental study on the failure of a novel composite sandwich structure. *Compos. Res.* **2016**, *29*, 209–215. [CrossRef]
18. Austermann, J.; Redmann, A.; Dahmen, D.; Quintanilla, A.; Osswald, T. Fiber-reinforced composite sandwich structures by co-curing with additive manufactured epoxy lattices. *J. Compos. Sci.* **2019**, *3*, 53. [CrossRef]
19. Hamed, E.; Negru, D.; Yalda, R. Structural performance of precast concrete sandwich panels made with FRP vierendeel truss-like connectors. *J. Compos. Constr.* **2022**, *26*, 04022027. [CrossRef]
20. Zhang, J.; Hu, X.; Hong, W.; Zhang, B.; Zhang, C. Experimental study on bending performance of composite sandwich panel with new mixed core. *MATEC Web Conf.* **2019**, *275*, 02018. [CrossRef]
21. Lee, J.H.; Kang, S.H.; Ha, Y.J.; Hong, S.G. Structural behavior of durable composite sandwich panels with high performance expanded polystyrene concrete. *Int. J. Concr. Struct. Mater.* **2018**, *12*, 21. [CrossRef]
22. Benayoune, A.; Samad, A.A.A.; Trikha, D.N.; Ali, A.A.A.; Ellinna, S.H.M. Flexural behaviour of pre-cast concrete sandwich composite panel—Experimental and theoretical investigations. *Constr. Build. Mater.* **2008**, *22*, 580–592. [CrossRef]
23. Chen, A.; Norris, T.G.; Hopkins, P.M.; Yossef, M. Experimental investigation and finite element analysis of flexural behavior of insulated concrete sandwich panels with FRP plate shear connectors. *Eng. Struct.* **2015**, *98*, 95–108. [CrossRef]
24. Barbu, L.G.; Oller, S.; Martinez, X.; Barbat, A. High cycle fatigue simulation: A new stepwise load-advancing strategy. *Eng. Struct.* **2015**, *97*, 118–129. [CrossRef]
25. Frankl, B.A.; Lucier, G.W.; Hassan, T.K.; Rizkalla, S.H. Behavior of precast, prestressed concrete sandwich wall panels reinforced with CFRP shear grid. *PCI J.* **2011**, *56*, 42–54. [CrossRef]
26. Carbonari, G.; Cavalaro, S.H.P.; Cansario, M.M.; Aguado, A. Flexural behaviour of light-weight sandwich panels composed by concrete and EPS. *Constr. Build. Mater.* **2012**, *35*, 792–799. [CrossRef]
27. Hou, H.; Ji, K.; Wang, W.; Qu, B.; Fang, M.; Qiu, C. Flexural behavior of precast insulated sandwich wall panels: Full-scale tests and design implications. *Eng. Struct.* **2019**, *180*, 750–761. [CrossRef]
28. Thoft-Chritensen, P.; Baker, M.J. *Structural Reliability Theory and Its Applications*; Springer: Berlin/Heidelberg, Germany, 1982. [CrossRef]
29. Wu, D.; Gao, W. Hybrid uncertain static analysis with random and interval fields. *Comput. Methods Appl. Mech. Eng.* **2017**, *315*, 222–246. [CrossRef]
30. Morales-Torres, A.; Escuder-Bueno, I.; Serrano-Lombillo, A.; Castillo Rodriguez, J.T. Dealing with epistemic uncertainty in risk-informed decision making for dam safety management. *Reliab. Eng. Syst. Saf.* **2019**, *191*, 106562. [CrossRef]
31. Capasso, V. Multiple scales and geometric structures: Additional sources of randomness. *J. Math. Biol.* **2009**, *59*, 143–146. [CrossRef] [PubMed]
32. Zhao, Y.-G.; Ang, A.H.S. On the first-order third-moment reliability method. *Struct. Infrastruct. Eng.* **2012**, *8*, 517–527. [CrossRef]
33. Yang, Z.; Ching, J. A novel simplified geotechnical reliability analysis method. *Appl. Math. Model.* **2019**, *74*, 337–349. [CrossRef]
34. Yang, Z.; Ching, J. A novel reliability-based design method based on quantile-based first-order second-moment. *Appl. Math. Model.* **2020**, *88*, 461–473. [CrossRef]
35. Moromi Nakata, I.; Garcia Fernandez, F.; Torre Carrillo, A.; Espinoza Haro, P.; Acuña Pinaud, L. Application of the Monte Carlo method to estimate the uncertainty in the compressive strength test of high-strength concrete modelled with a multilayer perceptron. *Rev. Constr.* **2018**, *17*, 319–329. [CrossRef]

36. Jiang, Y.; Zhou, H.; Wang, L.; Chen, Z.; Tang, T.; Adhikari, S. Reliability evaluation based on multiple response surfaces method considering construction uncertainties of cable tension for a hybrid roof structure. *ASCE-ASME J. Risk Uncertain. Eng. Syst. Part A Civ. Eng.* **2021**, *7*, 107401. [CrossRef]
37. Goswami, S.; Ghosh, S.; Chakraborty, S. Reliability analysis of structures by iterative improved response surface method. *Struct. Saf.* **2016**, *60*, 56–66. [CrossRef]
38. Straub, D.; Ehre, M.; Papaioannou, I. Decision-theoretic reliability sensitivity. *Reliab. Eng. Syst. Saf.* **2022**, *221*, 108215. [CrossRef]
39. Yang, Q.; Ma, H.; Ma, J.; Sun, Z.; Li, C. Sensitivity analysis of reliability of low-mobility parallel mechanisms based on a response surface method. *Appl. Sci.* **2021**, *11*, 9002. [CrossRef]
40. Lee, S. Reliability based design optimization using response surface augmented moment method. *J. Mech. Sci. Technol.* **2019**, *33*, 1751–1759. [CrossRef]
41. Radmehr, M.; Homami, P. The seismic reliability analysis of moment resisting frames with bolted end-plate connection. *J. Constr. Steel Res.* **2020**, *171*, 106134. [CrossRef]
42. Chun, J. Reliability-based design optimization of structures using complex-step approximation with sensitivity analysis. *Appl. Sci.* **2021**, *11*, 4708. [CrossRef]
43. Ding, Y.G.; Song, Z.J.; Chen, K.W.; Zhang, X.H. Thermal insulation performance and reliability of the "structure-insulation" integrated wall panel (SIW) for storage grain bungalows. *Buildings* **2022**, *12*, 1306. [CrossRef]
44. *GB50320-2014*; Code for Design of Grain Storehouses. China Planning Press: Beijing, China, 2014.
45. *GB/T50081-2019*; Standard for Test Methods of Concrete Physical and Mechanical Properties. China Architecture & Building Press: Beijing, China, 2019.
46. *GB50010-2010*; Code for Design of Concrete Structures. China Architecture & Building Press: Beijing, China, 2010.
47. Choi, I.; Kim, J.H.; Kim, H.R. Composite Behavior of Insulated Concrete Sandwich Wall Panels Subjected to Wind Pressure and Suction. *Materials* **2015**, *8*, 1264–1282. [CrossRef] [PubMed]
48. Choi, I.; Kim, J.H.; You, Y.C. Effect of cyclic loading on composite behavior of insulated concrete sandwich wall panels with GFRP shear connectors. *Compos. Part B* **2016**, *96*, 7–19. [CrossRef]
49. Taherinasab, M.; Aghakouchak, A.A. Parametric study on probabilistic local seismic demand of IBBC connection using finite element reliability method. *Steel Compos. Struct.* **2020**, *37*, 151–173. [CrossRef]
50. Asghshahr, M.S. Reliability Based Design Optimization of Reinforced Concrete Frames Using Genetic Algorithm. *Period. Polytech. Civ. Eng.* **2021**, *65*, 566–576. [CrossRef]
51. Onyeneke, C.C. A Modified Review and Proof of Central Limit Theorem in Relation with Law of Large Numbers. *Data Res.* **2018**, *2*, 111–119.
52. *GB50068-2018*; Unified Standard for Reliability Design of Building Structures. China Architecture & Building Press: Beijing, China, 2018.

Disclaimer/Publisher's Note: The statements, opinions and data contained in all publications are solely those of the individual author(s) and contributor(s) and not of MDPI and/or the editor(s). MDPI and/or the editor(s) disclaim responsibility for any injury to people or property resulting from any ideas, methods, instructions or products referred to in the content.